

**Dual-role electrolyte additive for simultaneous polysulfide shuttle inhibition and redox mediation in sulfur batteries**

Journal:	<i>Journal of Materials Chemistry A</i>
Manuscript ID	TA-ART-04-2021-003425.R2
Article Type:	Paper
Date Submitted by the Author:	05-Oct-2021
Complete List of Authors:	Rafie, Ayda; Drexel University, Chemical and Biological Engineering Pai, Rahul; Drexel University College of Engineering, Chemical and Biological Engineering Kalra, Vibha; Drexel University, Chemical and Biological Engineering

1 Dual-role electrolyte additive for simultaneous
2 polysulfide shuttle inhibition and redox mediation in
3 sulfur batteries

4 Ayda Rafie ^a, Rahul Pai ^a, and Vibha Kalra ^{a,*}

5 ^a Chemical and Biological Engineering, Drexel University, Philadelphia-19104, USA

6 *Corresponding author, Email: vk99@drexel.edu

7 Abstract

8 In Li-S batteries, the insulating nature of sulfur and Li₂S causes enormous challenges, such as
9 high polarization and low active material utilization. Nucleation of the solid discharge product,
10 Li₂S, during discharge cycle, and activation of Li₂S in the charge cycle, causes a potential barrier
11 that needs to be overcome. Moreover, shuttling of soluble lithium polysulfide intermediate species
12 results in active material loss and early capacity fade. In this study, we have studied thiourea as an
13 electrolyte additive and showed that it serves both as a redox mediator to overcome Li₂S activation

1 energy barrier, as well as shuttle inhibitor to mitigate the notorious polysulfide shuttling via
2 investigation of thiourea's redox activity, shuttle current measurements and study of Li_2S
3 activation. The steady-state shuttle current of Li-S battery shows a 6-fold drop when 0.02 M
4 thiourea is added to the standard electrolyte. Moreover, by adding thiourea, the charging plateau
5 for first cycle of the Li_2S based cathodes shifts from 3.5 V (standard ether electrolyte) to 2.5 V
6 (with 0.2 M thiourea). Using this additive, the capacity of Li-S battery stabilizes at ~839 mAh/g
7 after 5 cycles and remains stable over 700 cycles with a low capacity decay rate of 0.025% per
8 cycle, a tremendous improvement compared to the reference battery that retains only ~350 mAh/g
9 after 300 cycles. In the end, to demonstrate the practical and broad applicability of thiourea in
10 overcoming sulfur-battery challenges and in eliminating the need for complex electrode design,
11 we study two additional battery systems – lithium metal-free cells with graphite anode and Li_2S
12 cathode, and Li-S cells with simple slurry-based cathodes fabricated via blending commercial
13 carbon black/S and binder. We believe that this study manifests the advantages of redox active
14 electrolyte additives to facilitate several bottlenecks in the Li-S battery field.

15 **KEYWORDS:** Electrolyte additive, Redox mediator, Shuttle inhibitor, Redox active additives,
16 Polysulfide shuttle

1

2

3

4

5

6

7

8

9

10

11

12

13

14 1. Introduction:

15 Lithium-sulfur (Li-S) batteries are considered to be one of the most promising next generation

16 batteries owing to their high theoretical gravimetric energy density of ~2510 Wh/kg, and highly

17 abundant, cheap and non-toxic sulfur active material ¹. Nonetheless, there are challenges toward

1 commercialization of these batteries. The challenges on the cathode side are related to the
2 insulating nature of sulfur (S_8) and Li_2S , volume expansion ($\sim 80\%$) in each discharge, and most
3 importantly, the shuttling of intermediate polysulfides causing rapid capacity fade ¹⁻³. This past
4 decade has seen extensive research with exemplary works mitigating these challenges. Majority
5 of this research has been focused on cathode design involving 1) complex cathode architectures ⁴,
6 ⁵, 2) novel cathode host chemistries ⁶⁻⁸, and/or 3) modification of sulfur active material through
7 the formation of S-X covalent bond (where X can be carbon, metal, selenium, or phosphorus) ^{9, 10}
8 to enhance the conductivity, accommodate volume expansion and physically and/or chemically
9 entrap polysulfides.

10 However, an alternate and more economical solution is the engineering and design of electrolyte
11 additives. While often overshadowed by the overwhelming literature on cathode modifications,
12 electrolyte additives can play a vital role in enhancing the performance of Li-S batteries ¹¹⁻¹³. They
13 are usually added in very small fractions in the electrolyte and therefore, unlike cathode hosts, the
14 electrolyte additives would not typically hinder the achievable energy density of batteries ¹².
15 Moreover, efficient electrolyte additives can potentially eliminate the need for a complicated
16 cathode design ^{14, 15}. For these reasons, Li-ion industry heavily relies on electrolyte additives as

1 the most economical and efficient way to circumvent the issues and improve the battery
2 performance.

3 Nevertheless, research on electrolyte additives for Li-S batteries has been limited. In the Li-S
4 field, electrolyte additives with three primary roles have been investigated, all targeted toward
5 polysulfide shuttling– a) formation of a stable solid-electrolyte interphase (SEI) on the lithium
6 anode ¹⁶ to protect it from the shuttling polysulfides, b) development of a stable cathode electrolyte
7 interphase (CEI) to serve as a barrier to polysulfide diffusion at the cathode ¹², c) formation of
8 complexes with intermediate polysulfides to decrease polysulfide shuttling ¹⁷. The most commonly
9 used additive in Li-S batteries, LiNO₃, is believed to reduce the adverse effects of polysulfide
10 shuttling by formation of a protective SEI layer on Li metal anode ¹⁶. Such SEI formation on the
11 lithium anode has also been explored using other additives such as LiI and P₂S₅ ¹⁸. In addition,
12 additives such as fluorinated ethers or pyrrole can form a stable cathode electrolyte interphase
13 (CEI) on the sulfur cathode and perform as a barrier layer to suppress the diffusion of soluble
14 polysulfides ¹². Another interesting example of additives used to improve the cycling stability of
15 Li-S batteries is thiol-based additives, such as biphenyl-4,4'-dithiol (BPD) ^{13, 17}. Being a redox
16 active additive in the Li-S battery voltage range (1.8-2.6 V vs. Li/Li⁺), this additive forms BPD-

1 polysulfide complexes during the discharge step. The formation of such complexes results in
2 changes on the reduction pathways and mechanisms of sulfur cathodes. Nevertheless, each of the
3 additives studied play a single role limited to mitigation of polysulfide shuttling.

4 Overall, with limited literature on Li-S battery additives, there is a need to expand the spectrum
5 of additives that can play additional roles in mitigating Li-S chemistry challenges to truly eliminate
6 the need for complex/expensive cathode design. To this end, in this work, we demonstrate thiourea
7 as an additive that plays a “dual” role as both a polysulfide shuttle inhibitor and also as a redox
8 mediator (RM). A redox mediator, if successful, can dramatically increase the electron transfer
9 between the conductive host and active material without the need for physical contact, resulting in
10 enhanced active material utilization ^{19, 20}. While RM-type additives have been widely used in Li-
11 air batteries for Li_2O_2 utilization in each cycle ²¹, only a handful of reports investigate this concept
12 in Li-S batteries ^{15, 22}. Moreover, to the best of our knowledge there is no study in literature, where
13 an additive is used simultaneously both as a redox mediator and as a polysulfide shuttle inhibitor.
14 TU has been previously used as an electrolyte additive to Li-air batteries, and the SEI formation
15 with and without thiourea is investigated. In this work by Ho et al., the effect of TU on suppressing

1 the growth of Li dendrites is attributed to reduction in electrolyte decomposition in presence of
2 TU additive ²³.

3 In this work, we investigate thiourea as an organic electrolyte additive in Li-S batteries. The
4 major part of the study is focused on lithium-sulfur cells composed of lithium anode and
5 freestanding carbon nanofiber-based (CNF) sulfur cathode. On addition of thiourea into the
6 standard ether electrolyte, the cycle stability was increased by more than two-fold. Freestanding
7 binder-free and current collector-free CNF was used as a cathode sulfur host to prevent interference
8 from binders and/or current collectors in revealing the fundamental mechanism of TU activity in
9 sulfur batteries. Through an investigation of TU redox activity, shuttle current measurements, and
10 study of Li₂S activation, we show that thiourea serves as both a PS shuttle suppressing- and a redox
11 mediating-additive. We discuss in the paper that TU facilitates shuttle suppression through
12 formation of complexes between $C - S^{\cdot}$ and polysulfide anion radicals. To demonstrate TU's role
13 as a redox mediator, we synthesized Li₂S cathode (instead of sulfur) and showed that thiourea
14 reduced the activation potential of Li₂S, an ionically and electronically insulating material, from
15 3.4V to 2.54V.

1 In the final part of this work, we study two additional battery/material systems to demonstrate
2 the broad and practical applicability of thiourea additive enabling cheaper, and simpler electrodes
3 – in the first example, TU enables a stable lithium metal-free battery composed of commercial
4 graphite anode and Li_2S nanofiber cathode with a stable capacity of 900 mAh/g for 400 cycles. In
5 the second example, we show both coin cell and prototype-level pouch cell data where TU enabled
6 stable capacity for hundreds of charge-discharge cycles with simple industry-friendly slurry sulfur
7 cathodes (made by just blending commercial sulfur with carbon black and PVDF binder), which
8 are otherwise known to exhibit rapid capacity fade.

9 This work is the first ever study on the use of an electrolyte additive that enhances the
10 performance of Li-S batteries as both shuttle inhibitor and redox mediator. These results are a
11 significant initial step toward further studies on engineering electrolyte additives with multiple
12 roles.

13 2. Experimental Methods

14 2.1. Fabrication of SCNF/S and Li_2S /CNFs cathodes

15 We used electrospinning technique to fabricate carbon nanofibers (CNFs). The polymeric
16 solution for electrospinning was prepared by dissolving polyacrylonitrile (PAN, average MW:

1 150,000 Sigma-Aldrich) and dried LIQION (Nafion, Liquion 1105, Ion Power Inc.) in ratio of
2 40:60 wt% in N,N-dimethylformamide (DMF, Sigma Aldrich)²⁴. The total solid concentration of
3 18% was used to prepare the solution. This solution was then loaded into the syringes and
4 electrospun using a 22-gauge needle (stainless steel needle, Hamilton Co.). The electrospinning
5 was carried out using the following conditions: flowrate was set 0.2 mL/h, the distance between
6 the needle and Al foil collector was adjusted between 15 to 16 cm, and the voltage was set between
7 9 to 10 kV to ensure smooth electrospinning. Electrospinning was carried out at room temperature,
8 and the humidity electrospinning chamber was kept below 20% using zeolite desiccants. The
9 electrospun nanofiber mats were then stabilized at 280 °C for 6 h under air in a convection oven
10 (Binder Inc, Germany). The stabilized samples were then carbonized in a tube furnace (MTI Co.,
11 USA) at 1000 °C for 1 h under continuous N₂ flow. The heating rate of the furnace was adjusted
12 to 3 °C/min both for heating and cooling steps. To incorporate sulfur, we used the “ultra-rapid melt
13 diffusion” technique, developed in our lab²⁵. In this technique, a desired amount of sulfur is
14 sprinkled on CNFs, and a hot press was used to incorporate sulfur into the CNFs matrix at 155 °C
15 for only 55 sec using a slight pressure of < 250 psi. The Li₂S/CNF cathodes were synthesized by
16 electrospinning a mixture of 0.5 g Li₂SO₄ (Sigma Aldrich), and 1g Polyvinylpyrrolidone (MW:

1 300,000, Sigma Aldrich) in a mixture of 4.5 g DI water, 3 g ethanol/, and 1.5 g acetone solvents.
2 The electrospun fiber mats were then stabilized at 170 °C for 20 h under air and carbonized at 900
3 °C for 1 h under continuous flow of Ar. The nanofibers were immediately transferred to glovebox
4 antechamber after the heat treatment to avoid any exposure to air.

5 2.2. Characterization of Cathodes

6 Thermogravimetric analysis (TGA) on sulfur powder and SCNF cathode was carried out on a
7 TA 2950 (TA Instruments, USA), under a steady flow of N₂. A very slow heating rate of 2.5°C/min
8 was used to increase temperature from room temperature to 800 °C. To measure the Li₂S content
9 of Li₂S/CNF samples, anhydrous methanol was used to wash away the Li₂S particles and the
10 weight of the sample was measured before and after the washing procedure. The measurements
11 were carried out on three samples from three different batches, and the 46.2 wt% of the Li₂S
12 particles were calculated based on the weight difference measured. The formation of Li₂S is
13 confirmed using X-ray diffraction (XRD), collected using a Rigaku MiniFlex 600. The Li₂S
14 samples were sealed inside the glovebox using Kapton tape to avoid air exposure while transferring
15 to XRD. The morphology of CNFs, Li₂S/CNFs, and SCNFs are investigated using The Zeiss Supra
16 50VP field-emission scanning electron microscope (SEM). The SEM instrument was equipped

1 with an Oxford UltiMax 40 mm energy dispersive spectrometer (EDS), used for elemental
2 mapping. A very thin layer of platinum was sputtered using a Cressington sputter coater to increase
3 the conductivity of samples. The Li_2S samples were transferred using an air-tight container, sealed
4 inside the glovebox, however, the samples were exposed to air for a very short period of time (~
5 30 s) before transferring to the SEM chamber. To collect the infrared spectra of the electrolyte
6 with TU additive before and after exposure to Li metal, we used a Fourier transform infrared
7 (FTIR) spectrometer (Nicolet iS50, Thermo-Fisher Scientific), equipped with an extended range
8 diamond ATR accessory and with a deuterated triglycine sulfate (DTGS) detector. The FTIR puck
9 was transferred to glovebox and 60 μL of the sample was used and sealed under Ar to avoid
10 ,moisture and oxygen contamination. The spectra were collected with a resolution of 64 scans per
11 spectrum at 8 cm^{-1} , and they were corrected using background, baseline correction and advanced
12 ATR correction in the Thermo Scientific Omnic software package.

13 2.4. Coin cells and pouch cell fabrication and electrochemical testing

14 The $\text{Li}_2\text{S}/\text{CNFs}$ cathode was used without any further modification. The CNF cathodes (without
15 any sulfur active material) were dried at $140\text{ }^\circ\text{C}$ overnight using a convection oven. The SCNF
16 cathodes were then dried under vacuum before transferring them inside the glovebox. The

1 $\text{Li}_2\text{S}/\text{CNF}$, CNFs, and SCNFs were used without using any binder or current collectors. For slurry
2 cathodes, sulfur, PVDF binder, and super p conductive carbon was used in weight ratio of
3 50:10:40. A proper amount of NMP solvent was used and the solution was stirred overnight using
4 a stirring plate. The slurry was then coated on an Al foil with different thicknesses using a doctor
5 blade. The thickness of coating was changed to achieve a loading of 1.6 to 5 mg/cm^2 of sulfur.
6 Slurry cathodes were then dried overnight under air and at 55 °C, and for 12 h under vacuum. The
7 area of both freestanding and slurry cathodes was 0.855 cm^2 . To fabricate the coin cells, we used
8 the CR2032 coin cells, stainless steel spacers and springs (all from MTI corporation), Li foil
9 (Aldrich, punched to 13 mm diameter discs) as anode, $\text{Li}_2\text{S}/\text{CNFs}$, SCNFs, CNFs and sulfur slurries
10 as cathode and a polypropylene separator (Celgard 2500; 19 mm diameter). To synthesize the
11 ether-based electrolyte, we mixed 1.85 M LiCF_3SO_3 (99.995% trace metals basis, Sigma Aldrich)
12 as salt, 0.1 M LiNO_3 (Acros Organics) (as an additive). The salt and additive used in this study
13 were transferred to the glove box upon receiving without any further modification. We used a
14 solution of 1,2-dimethoxyethane (DME, Acros Organics) and 1,3-dioxolane (DOL, Sigma
15 Aldrich) at a 1:1 volume ratio as solvents. To synthesize ether-based electrolyte with TU additive,
16 we added a proper amount of thiourea (Sigma Aldrich) to achieve concentration of 0.02 M, 0.2 M

1 and 0.5 M in the electrolyte. The amount of electrolyte used in coin cells was set to 30 μL for all
2 the SCNFs and slurry-based cathodes except for the high loading cells (between 4 to 5 mg/cm^2).
3 The amount of electrolyte used for these cells was 80 μL . All the coin cells were rested for 4 hours
4 at their open circuit voltage, and conditioned at C/10 and C/5 (two cycles at each rate) before long-
5 term cycling at C/2 between 1.8 to 2.7 V (vs Li/Li⁺). For cells cycled at C/5 we conditioned the
6 cells at C/20 and C/10 (for two cycles). Likewise, for cells cycled at C/10 we conditioned the cells
7 at C/20 for two cycles. For the Li-S pouch cell, we have used the slurry-based cathode (25 cm^2)
8 with Li metal foil anode rolled on a copper foil. We used ether electrolyte with 0.2 M TU additive
9 and sealed the pouch cell package under vacuum. In all the electrochemical testing where sulfur is
10 used as the active material, 1C is 1675 mAh/g and all the reported discharge capacities in the
11 manuscript are based on the sulfur weight. For the coin cells fabricated using Li₂S/CNFs as the
12 cathode material, cells were first charged to 3.8 V for the first cycle at C/20, following with
13 condition cycles at C/10, and C/5 and long-term cycling at C/2 rate between 1.8 to 2.7 V. The Li
14 metal-free coin cell was fabricated using Li₂S/CNFs as cathode and graphite (single layer graphite
15 coated on copper foil, MTI corporation) as anode. The graphite electrodes were used after drying
16 overnight in vacuum, without any further modification. In all these coin cells, 1C is considered as

1 the theoretical capacity of Li_2S (~ 1166 mAh/g) and the discharge capacity reported is based on the
2 weight of Li_2S in cathode. Long-term cycling of the batteries was carried out using a MACCOR
3 (4000 series) battery cyler and Neware battery cyler. For shuttle current measurements we
4 cycled the cells for 3 cycles and stopped them at the desired voltage in the discharge step. To
5 compare the shuttle currents, we used coin cells with 0 M (as reference), 0.02 M and 0.2 M TU
6 additive and measured the shuttle current at 4 different potentials. For example, for the cells
7 stopped at 2.3 V, we applied a constant potential of 2.3 V, and held the cell at this potential for 2
8 h and recorded the current response. The shuttle current measurements and cyclic voltammetry
9 (CV) tests were carried out using a potentiostat (Gamry reference 1000).

10 3. Results and Discussion

11 *Redox activity of thiourea*

12 Figure 1a shows the SEM image of CNFs used as cathode material in these cells. The fabrication
13 method has been described in the experimental section. The freestanding nature of the CNFs does
14 not require the use of any binders or Al current collectors. To incorporate sulfur, we used the
15 “ultra-rapid melt diffusion” technique developed in our lab²⁵. In this technique, a desired amount
16 of sulfur is sprinkled on CNFs and incorporated into the nanofibers mat using a hot press in only

1 55 s. The SEM images of SCNF cathodes used in this study are presented in figure 1b. The cross-
2 section SEM pictures and elemental mapping of SCNF cathodes are shown in the supplementary
3 information, figure S1. The elemental mapping in this figure confirms that sulfur is incorporated
4 throughout the CNF mat thickness. To confirm the sulfur weight percent, TGA curve of the SCNF
5 cathode is presented and compared to the TGA plot of pure sulfur in figure 1c. The TGA results
6 show that sulfur weight % in the SCNF cathode is ~48%. A slight shift is observed in the
7 decomposition temperature of sulfur in SCNF cathode compared to pure sulfur powder. A similar
8 trend was reported by our group in previous studies, where sulfur or sulfur-rich copolymers were
9 used as active material and incorporated into the CNFs using a hot press ^{5, 25}. We believe that the
10 slight shift is related to the enhanced heat transfer as a result of increased surface area, which
11 results in a lower decomposition temperature. The CNFs and SCNFs were dried under vacuum
12 and used as cathode without any further modification.

13 To understand the effect of thiourea-based electrolyte additive in the performance of Li-S
14 batteries, we first fabricated coin cells using CNFs as cathode (without any sulfur active material).
15 These coin cells are referred to as “blank cells” in the manuscript and serve as reference cells to
16 first understand thiourea activity without the interference of sulfur active material and eventually

1 elucidate its interaction with polysulfides when sulfur is added. Figure 2a shows the cyclic
2 voltammetry (CV) of the blank cells with and without thiourea additive. The black line is a blank
3 cell with the conventional ether-based electrolyte without thiourea. The other CVs in figure 2a are
4 for similar coin cells at a scan rate of 0.02 mV/s, when 0.02 M TU is added to the electrolyte. As
5 can be seen in this figure, two pairs of redox peaks, denoted as A/A' and B/B', appear when TU
6 is added to the electrolyte. The reduction peaks at ~2.4 (denoted as A) and ~2.0 V (denoted as B)
7 and oxidation peaks at ~ 2.2V (denoted as B') and ~2.4 V (denoted as A') confirm that TU has a
8 redox activity in ether-based electrolyte. Note that the peaks are consistently present over five
9 cycles, with almost same intensity, confirming the reversible nature of the redox behavior of TU.
10 TU is known to have redox activity in aqueous acidic or alkaline media²⁶⁻³⁰, however, to date there
11 is no report focusing on the reversible redox activity of TU additive in non-aqueous environment.
12 Figure 2b shows the effect of scan rate on the CV result of coin cells with TU additive. The two
13 redox peaks are still present at high scan rate of 0.5 mV/s. Further increase in the scan rate results
14 in vanishing of the second cathodic peak (see figure S2a). At higher scan rates, the anodic peak at
15 ~2.2 V shifts to ~2.35 V and its intensity becomes very low. Following these experiments, we also
16 carried out cyclic voltammetry experiment over an extended potential range, from 1.4 V to 3V at

1 0.1 mV/s. The result of this experiment is presented in figure S2b. Bercot et al, reported that TU
2 has an irreversible redox reaction in acetonitrile solvent ²⁷. Based on our results, there are two
3 reversible redox pairs, and no irreversible reduction or oxidation peak was observed.

4 To understand the effect of TU concentration, we fabricated blank coin cells using 0.02 M, 0.2
5 M and 0.5 M thiourea additive. Figure 2c, shows the CV results of these coin cells. It is clear from
6 this figure that the intensity of the redox peaks becomes stronger as thiourea concentration
7 increases, corroborating the peaks are indeed associated with TU redox activity. To have a better
8 understanding of the effect of TU additive, we have adjusted the y axis (current) in figure 2a and
9 2c based on the amount of TU used in the battery, see figure S2c and S2d. As can be seen in figure
10 S2d, when current is adjusted based on the weight of TU used in the cell, very similar current
11 response is measured. We believe that as a result of electrochemical reactions happening at the
12 electrode-electrolyte interface, thiourea reversibly converts to formamidine disulfide. The
13 structure of thiourea, formamidine disulfide (FDS) and a hypothesized reaction pathway are
14 presented in figure 2d. To confirm this hypothesis, we fabricated a slurry using commercial
15 formamidine disulfide as active material. The slurry was composed of formamide disulfide, PVDF
16 and conductive carbon. The FDS cathode was used without further modification in ether-based

1 electrolyte (without TU additive). Figure S3a shows the CV results for FDS in ether-based
2 electrolyte. As shown in this figure, two redox peaks in cathodic and anodic scans are present. The
3 reduction peaks at ~ 2.39 V and ~ 2.1 V are very similar to the peaks shown in figure 2a in the
4 presence of TU. Moreover, the oxidation peaks at ~ 2.3 V and ~ 2.4 V are in similar position as the
5 TU redox peaks; however, the intensity of the peaks seems to be different. Based on the similarities
6 in the CV results of TU and FDS, we hypothesize that the TU additive reversibly converts to FDS.
7 We also carried out FTIR experiments of the electrolytes with TU after exposure to Li metal. Based
8 on the results presented in figure S4, thiourea molecules are not lithiated after exposure to Li metal.
9 We believe that the redox behavior of TU is originated from the sulfur atom being oxidized and
10 thereby, a dimer is formed. The reduced sulfur atom forms a bond with another reduced sulfur
11 atom, forming a disulfide bond (figure 2d). The disulfide is then reduced to its original state at the
12 discharge. TU exists as a hybrid of different resonance mesomers, presented in figure S3b³¹. The
13 contribution of different mesomers is known to be affected by pressure, temperature or solvents
14³². As a result of this resonance, the negative charge of the sulfur atom in its reduced condition is
15 not localized, so the electrochemical reaction is accelerated. This phenomenon can explain the
16 electrochemical reaction of thiourea at high scan rates up to 10 mV/s. Similar electrochemical

1 pathways have been reported in the literature for thiourea-based materials. Hiroshi et al. reported
2 the electrochemical activity of sulfur atom in thiourea or/and polymers with thiourea as its main
3 polymeric unit ³¹. This study investigated thiourea-based compounds as electrode material in
4 lithium secondary batteries using a gel polymer electrolyte. Based on this report, the sulfur atom
5 in thiourea is responsible for the reversible electrochemical reactions by forming a disulfide bond
6 with sulfur from another TU compound. The result of this study is in agreement with our
7 hypothesis of formation of the C-S bond when TU is used as an additive and cycled in the battery.

8 *Effect of thiourea additive on the performance of Li-S batteries*

9 To demonstrate the effect of TU additive on the performance of Li-S batteries, the same
10 freestanding SCNF cathodes, used for the redox activity study above, with loading of 1.2 to 1.4
11 mg/cm² were used. To evaluate the effect of thiourea additive, we fabricated cells using 0 M (i.e
12 ether electrolyte without TU as a reference), 0.02 M, and 0.2 M TU. Figure 3a, shows the CV
13 results for these batteries. As can be seen from CV results, the reference electrolyte shows two
14 typical reduction peaks. The first one corresponds to formation of long chain polysulfides (Li_2S_x ,
15 $6 \leq x \leq 8$) and the second one corresponds to the conversion of long chain polysulfide to short chain
16 polysulfides (Li_2S_x , $x < 6$), and their final conversion to the Li_2S solid discharge product. The two

1 reduction peaks appear at ~ 2.30 V and ~ 1.95 V in the reference cell (i.e., ether-based electrolyte
2 without TU additive). When TU additive was added to the electrolyte, there is a clear shift toward
3 higher voltage in each reduction peak of the Li-S battery. For the coin cell with 0.2 M TU (blue
4 line in figure 3a), the first reduction peak appears at ~ 2.34 V and the second peak at ~ 2.02 V,
5 corresponding to ~ 400 mV and ~ 70 mV shift from the reference cell, respectively. Moreover, a
6 small shoulder is seen in the second reduction peak, which might be originating from the redox
7 activity of TU additive. The broad oxidation peak, on the other hand, shifted toward a lower
8 voltage, when TU additive was used. Based on the CV results in figure 3a, TU additive decreases
9 the polarization of the cell, possibly by facilitating the deposition of Li_2S (in the discharge process),
10 and utilization of Li_2S (in the charging process) of the battery. These results are interesting because
11 the addition of TU to electrolyte is expected to decrease the ionic conductivity of electrolyte, which
12 in fact can have the opposite effect of increased cell polarization. Ho et al., for example, showed
13 that the ionic conductivity at room temperature of an ether-based electrolyte was decreased from
14 $\sim 1.2 \times 10^{-5}$ S/cm to $\sim 1.0 \times 10^{-5}$ S/cm in the presence of 1.0 M TU additive²³. The decrease in
15 polarization of the battery, despite the increase in electrolyte resistance, confirms that TU additive

1 can facilitate the kinetics of redox reaction in Li-S batteries. We believe that TU can act as a redox
2 mediator (discussed later) to enhance the kinetics of Li-S batteries.

3 The long-term cycling result of batteries with and without TU additive is presented in Figure 3b.
4 All cells were conditioned at C/10 and C/5 rates for two cycles each, before long-term cycling at
5 C/2 (where 1C=1675 mAh/g). As can be seen in this figure, the capacity of reference Li-S battery
6 (with ether-based electrolyte without TU additive) continuously decreases within 300 cycles. On
7 the other hand, cells with only 0.02 M TU additive show relatively stable cycling up to 300 cycles
8 with the capacity being at ~ 525 mAh/g after 300 cycles. Further increase in TU concentration
9 results in a very stable cycling with higher capacity compared to previous cells. The coin cell with
10 0.2 M TU additive, showed a capacity of ~780 mAh/g after 300 cycles. The long-term cycling of
11 the coin cell with 0.2 M TU up to 700 cycles additive is presented in figure 3c. The capacity of
12 this cell was stabilized to 839 mAh/g after 5 cycles with a capacity decay rate of 0.025 % per cycle
13 and with a coulombic efficiency of more than 97% throughout the cycling. Moreover, as
14 mentioned earlier. TU is a redox active material in potential window of Li-S battery, therefore, to
15 calculate the contribution of this additive to the capacity of the batteries, we have calculated the
16 theoretical capacity of TU based on $1e^-$ transfer per mole of TU, and adjusted this number based

1 on the g of active material used. Our calculations, presented in supplementary data, shows that the
2 0.02 M and 0.2 M TU added to the reference ethe electrolyte, can contribute up to 10.72 mAh/g
3 and 107.2 mAh/g and 268 mAh/g, respectively.

4 Based on the electrochemical results discussed so far, we can conclude that TU additive can
5 have a tremendous effect on decreasing the cell polarization and enhancing the capacity and cycle
6 life of Li-S batteries. We believe that these improved results can be attributed to the dual role of
7 TU additive in Li-S batteries. The first role is the positive effect of TU as a shuttle inhibitor. TU
8 can be used to control and delay the polysulfide shuttle phenomena. Moreover, we hypothesize
9 that this additive can act as a redox mediator to facilitate the kinetics of the reaction in each
10 discharge and charge half cycles. To investigate our hypothesis, we designed a series of
11 electrochemical experiments, as discussed below. To show TU'S effect on reducing the
12 polysulfide shuttling, we measured the steady-state shuttle current of Li-S batteries with and
13 without TU additive. To confirm the role of TU as a redox mediator, we synthesized Li_2S decorated
14 carbon nanofibers ($\text{Li}_2\text{S}/\text{CNFs}$) and used them as a cathode in Li-S battery (without any additional
15 sulfur). We then compared the Li_2S activation in the first charging step, with and without TU
16 additive.

1 *Thiourea as a shuttle inhibitor additive*

2 The long cycle life of a Li-S battery, along with the high coulombic efficiency throughout the
3 cycling, are considered to be indicators of shuttle control in Li-S batteries ^{1, 33} Mikhaylik et al.,
4 attempted to quantify the redox shuttle in Li-S batteries using a combination of mathematical
5 models and experimental results, introducing the “charge-shuttle factor” ³⁴. More recently, a new
6 electrochemical approach, termed as the “steady-state shuttle current” measurement, was
7 introduced by Moy et al. ³⁵. This simple but direct measurement of the shuttle current provides a
8 better insight into the effect of using different additives or host materials to control the PS shuttle
9 challenge ³⁶⁻³⁸. The overall idea behind this measurement relies on the decrease in the cell potential
10 as a result of the polysulfide diffusion from cathode to anode. Hence, the shuttle current is basically
11 the faradic current needed to balance the polysulfide shuttle from cathode to anode. We fabricated
12 coin cells with different concentration of TU, starting from 0 M (reference cell) to 0.02M and 0.2
13 M TU. The cells were cycled for three cycles at 0.1 mV/s and stopped at various potentials. The
14 cell potential was then kept constant at the corresponding potential and the current response was
15 recorded using a potentiostat. This experiment was repeated at 4 different potentials. It is important
16 to note that to avoid any false results, we have used cathodes with similar sulfur loading and wt%.

1 This is because the polysulfide concentration at each given voltage strongly depends on the sulfur
2 loading, and the measured shuttle current is a representation of the concentration gradient across
3 the cell. Figure 4 shows the effect of TU concentration on the shuttle current measured at 2.3V for
4 2 hours. The shuttle current measurement at ~2.3 V corresponds to the formation of Li_2S_6 , which
5 is known to be the most soluble polysulfide specie in ether-based electrolyte and can give valuable
6 information. As can be seen in figure 4, there is a transient region which arises from the small
7 difference between the open circuit voltage of the cell and the potential at which the measurement
8 is carried out. This transient region is followed by a steady state region, known as the shuttle
9 current. The measured shuttle current drops from ~0.6 mA/cm² to ~0.1 mA/cm² in presence of 0.02
10 M TU, which is almost 6-fold drop in the shuttle current measured at 2.3 V. Moreover, by
11 increasing the TU concentration to 0.2 M, the measured shuttle current further decreases to almost
12 zero. Based on the discussion presented, the decrease in the shuttle current in presence of TU
13 additive is a direct sign of a reduced polysulfide shuttle. Moreover, as can be seen in figure 4, the
14 shuttle current gradually decreases when no TU is used, however, when 0.2 M TU is added to the
15 electrolyte, the shuttle current remains very stable for two hours. The gradual decrease in the
16 measured current show that the concentration gradient changes over time. This decrease can be

1 attributed to the formation of insoluble products on anode side ³⁵. Figure S5 a-c presents the shuttle
2 current measurement at 2.1 V, 2.0 V, and 1.9 V. The negative sign in the shuttle current,
3 corresponds to the beginning of formation of the insoluble products. The appearance of the
4 negative sign at 2.1 V only for 0.2 M TU, confirms that the formation of insoluble products (at the
5 second peak in CV results) occurs earlier when 0.2 M TU is used. This results further confirm the
6 conclusions from CV results discussed before. We believe that there are three possible ways in
7 which TU can bind lithium polysulfides and reduce their shuttling during cycling of the Li-S
8 batteries. The C=S and the amine functional group in TU additive can bind lithium polysulfides
9 formed during discharge. For example a binding energy of ~1.13 eV is reported between nitrogen
10 in amine group and Li₂S via polar-polar interaction ³⁷. Moreover, as discussed before, the FDS
11 formation as a result of electrochemical oxidation of TU additive can also contribute to binding of
12 PSs. Once the S-S bond in FDS (C-S-S-C) breaks, the two radicals formed at the terminal sulfurs,
13 connected to carbon, can bind the S₃⁻ formed in the discharge process of Li-S batteries. A similar
14 binding mechanism is reported previously using thiol-based additives for Li-S batteries ¹⁷.

15 *Thiourea as a redox mediator additive*

1 Apart from this additive's positive role in inhibiting the PS shuttling, we believe that the TU can
2 also serve as a redox mediator to enhance the kinetics of reactions. RMs can accelerate the kinetics
3 of the reaction and improve the performance of batteries by utilizing the active material in each
4 charge and discharge half cycles^{15, 22, 39}. The use of redox mediators in Li-S batteries becomes
5 vital as the Li₂S discharge product is ionically and electronically insulating⁴⁰⁻⁴². As a result, a large
6 overpotential is needed to overcome the energy barrier of Li₂S. We believe that TU as a redox
7 mediator can help re-utilize the Li₂S particles that are not in direct contact with conductive host
8 material, here CNFs. To investigate this hypothesis, we have synthesized Li₂S/CNFs cathode
9 material, using electrospinning. We adopted and modified a previous method report in the
10 literature to fabricate the Li₂S-based cathodes outside the glovebox⁴³. PVP was used as the carbon
11 source and Li₂SO₄ as a precursor to synthesize Li₂S using a thermal treatment ($Li_2SO_4 + 2C \rightarrow Li_2$
12 $S + 2CO_2$). It is worth mentioning that by using electrospinning, all the synthesis procedure was
13 carried out outside the glovebox and the nanofibers were transferred inside right after the final heat
14 treatment under argon flow. Figure 5a and b show the SEM picture of the Li₂S/CNFs and their
15 elemental mapping. As can be seen in this figure, the Li₂S/CNF cathode material has a porous
16 structure which can help in Li₂S utilization. The porous structure of this material might be a result

1 of using acetone as a cosolvent in electrospinning. A similar result is reported by Megleski et al.,
2 examining the properties of electrospun polyester fibers using various ratios of DMF (less volatile)
3 and THF (more volatile)⁴⁴. Based on the result of their study, a vapor-induced phase separation is
4 responsible for the pore formation. The formation of pore is determined by the vapor pressure (or
5 boiling point) of the nonsolvent and polymer concentration. The sulfur elemental mapping
6 confirms that Li_2S particles are uniformly distributed in the $\text{Li}_2\text{S}/\text{CNF}$ cathode material. Moreover,
7 the formation of Li_2S decorated CNFs is confirmed using XRD. Figure 5c shows the XRD results
8 of the $\text{Li}_2\text{S}/\text{CNF}$ cathode. To carry out this experiment, we sealed the $\text{Li}_2\text{S}/\text{CNFs}$ using Kapton
9 tape inside the glovebox. The XRD of Kapton tape is also presented in figure 5c as a reference and
10 it confirms that the Kapton tape is responsible for the hump at ~ 18 degrees and the crystalline
11 peaks are solely from the presence of Li_2S particles. As can be seen in figure 5c, the 2θ peaks at
12 $\sim 26, 32, 45, 53,$ and 58 degrees confirm the formation of Li_2S decorated CNFs. To confirm that
13 TU additive can be used as a RM to facilitate Li_2S utilization, we fabricated coin cells using
14 $\text{Li}_2\text{S}/\text{CNFs}$ as the cathode, and we compared the electrochemical results with and without addition
15 of TU additive. The $\text{Li}_2\text{S}/\text{CNF}$ based coin cells were charged to 3.6 V at C/20 rate ($1\text{C}=1166$
16 $\text{mAh/g}_{\text{Li}_2\text{S}}$), to compare the utilization of Li_2S and its conversion to S_8 . It is worth mentioning that

1 the redox activity of TU is at a slightly higher voltage than the theoretical potential for Li_2S
2 oxidation (~ 2.15), which makes it an ideal candidate for a redox mediator¹⁵. Figure 6a shows the
3 galvanostatic charging for the first cycle of the batteries using Li_2S as cathode material. As can be
4 seen from this figure, the activation overpotential for a conventional Li_2S -based cathode is not
5 observed in our results. The mitigation of such overpotential might originate from nanofibrous
6 morphology and enhanced surface area of $\text{Li}_2\text{S}/\text{CNFs}$. Nevertheless, there are clear differences
7 between the voltage plateaus in presence of TU additive. The cell without an additive shows a
8 small potential plateau at ~ 2.9 V followed by a larger plateau at ~ 3.5 V, with most of the capacity,
9 or Li_2S activation originating from the second plateau. However, by adding 0.2 M TU, the plateau
10 contributing for Li_2S activation shifts to ~ 2.5 V. In other words, if the cut-off voltage of cells with
11 $\text{Li}_2\text{S}/\text{CNFs}$ were set to 3.0 V, the capacity of cell with TU would be ~ 679 mAh/g, whereas the
12 reference cell without TU additive would only have a capacity of ~ 183 mAh/g. The battery with
13 0.2 M TU as an additive shows the capacity of 1080 mAh/g, which is clearly higher than the battery
14 without TU additive (~ 620 mAh/g) in the first charging step. Figure 6b is the charge-discharge
15 curves of $\text{Li}_2\text{S}/\text{CNF}$ cathode after the activation step (first discharge), which shows the two-
16 potential plateau behavior of $\text{Li}_2\text{S}/\text{CNF}$ cathode with and without TU additive in Li-S battery.

1 However, similar to the charging step, the first discharge capacity of $\text{Li}_2\text{S}/\text{CNFs}$ cathodes was
2 enhanced from 588 mAh/g to 1005 mAh/g by adding 0.2 M TU to the reference ether electrolyte.
3 The role of TU in facilitating this conversion is not limited to the first cycle only. Based on these
4 electrochemical results, we believe that TU acts as a redox mediator to facilitate the conversion of
5 Li_2S to S. Schematic 1 shows the proposed dual role of TU as an additive to reduce the shuttling
6 of PSs and as a redox mediator in the discharge and charge step of Li-S batteries.

7 *Broad applicability of TU in development of practical cells*

8 In this final section, we demonstrate the broad applicability and benefit of thiourea in cells with
9 more practical cathode designs. In the first example, we built a lithium metal-free cell with a
10 commercial graphite anode, Li_2S -based cathode and 0.2M TU in standard ether electrolyte. This
11 cell retains a capacity of ~1007 mAh/g at C/2 rate after 400 cycles, 4-5-fold higher than typical
12 Li-ion battery cathodes. The cycling result of this cell is presented in figure S6 and shows the
13 potential of TU additive in enabling the combination of Li_2S cathode with a negative anode
14 material in a dry room without the need for anode lithiation⁴⁰. Such a battery could address all
15 safety concerns around the use of pure lithium anode, while still providing a capacity several fold
16 higher than the Li-ion batteries.

1 In the second example, we build lithium-sulfur cells using lithium metal anode, but a simple
2 slurry-based cathode fabricated via just blending commercial sulfur with carbon black and PVDF
3 binder. Although, slurry-based cathodes have the disadvantage of added weight because of the
4 insulating binder and current collector, however, they are commonly used in industry. Moreover,
5 numerous research papers have demonstrated rapid capacity fade in such cathodes in ether
6 electrolytes due to shuttling and will therefore serve as a great candidate to demonstrate the
7 practical advantage of thiourea additive and its applicability to various types of sulfur cathodes.
8 Our Li-S batteries fabricated using these cathodes with a loading of 1.4-1.6 mg/cm² showed a
9 stable capacity of ~575 mAh/g at C/2 rate even after 700 cycles when TU was added whereas the
10 reference battery without TU reaches ~150 mAh/g (figure 7a). The initial capacity drop observed
11 in figure 7a is a common observation in Li-S battery field. Although the exact reason behind this
12 initial capacity drop is unclear, however it can be attributed to the required time/cycles for
13 polysulfides to reach to equilibrium in the cell ^{45,46}. In addition Thieme et al., correlated the initial
14 drop to the E/S ratio and suggested that an optimum polysulfide concentration might help in
15 avoiding the irreversible loss and consequently the initial drop ⁴⁷. Moreover, we increased the
16 sulfur loading of the cell to 2-2.1 mg/cm² (see figure S7) and achieved a stable cycling up to 300

1 cycles. We conducted rate capability on these cells testing with rates all the way to 1C. The cells
2 without TU do not operate at such high rates, because of slow kinetics and high polarization ³³.
3 Figure 7b, shows the successful rate capability test using TU additive. Figure 7c shows cells with
4 practical sulfur loading of 4.7 mg/cm². They exhibit a capacity of ~730 mAh/g, which stabilizes
5 to ~525 mAh/g after 10 cycles and remains stable up to 250 cycles, with its coulombic efficiency
6 being ~97%. It is important to note that in literature, these slurry cathodes (carbon black/S/binder)
7 typically fail in less than 100 cycles, even with low S-loadings of ~1 mg/cm² ⁴⁸. The high loading
8 data is specifically important, because it is reported that sulfur loading of ~5-6 mg/cm² is required
9 to achieve an energy density of ~500 Wh/kg, which seems to be practically relevant result ^{19, 33, 49}.
10 Finally, we built prototype-level pouch cells with 25 cm² electrode area using slurry cathodes and
11 0.2 M thiourea (figure 7d). The initial increase in the capacity is possibly due to insufficient
12 electrolyte wetting in the large area cells. The pouch cell retained a capacity of ~601 mA/g after
13 10 cycles and remained stable up to 250 cycles with a low capacity decay rate of 0.042% per cycle.

14 4. Conclusions

15 In this study, we have introduced thiourea as a redox active electrolyte for Li-S batteries. Using
16 TU additive, the SCNF cathode showed a capacity of ~839 mAh/g after 5 cycles. This capacity

1 remained stable over 700 cycles with a low capacity decay of 0.025% per cycle and coulombic
2 efficiency of >97%. On the other hand, the capacity of the reference battery without TU additive
3 continuously dropped over 300 cycles. We demonstrated that the outstanding performance of
4 batteries with TU electrolyte originates from the dual role of this additive as a redox mediator and
5 shuttle inhibitor. To show the polysulfide suppression role of this additive, we used the steady-
6 state shuttle current measurements at four different discharge states. The shuttle current measured
7 showed a 6-fold decrease in the steady state shuttle current when only 0.02 M TU was added to
8 the ether-based electrolyte. Moreover, to show the redox mediation role of TU we fabricated cells
9 using Li_2S cathode, and showed a significant decrease in activation potential of Li_2S cathodes in
10 presence of TU. To further illustrate the broad application of these additives we have studied two
11 more systems. The first system is a Li metal-free cell, with graphite as anode and Li_2S as cathode
12 material. This cell shows a stable capacity of ~1007 mA/hg after 400 cycles. The second system
13 relies on using the simple industry-friendly carbon/sulfur slurry in coin cell and pouch cell level
14 Li-S battery. Our results show stable cycling of Li-S batteries with 25 cm^2 carbon/sulfur slurry
15 cathode over 250 cycles with capacity decay rate of 0.042 % per cycle. As indicated in this study,
16 on addition of only 0.2 M TU, a significant improvement in practical Li-S batteries is achieved.

1 To demonstrate the significant role of thiourea additive in improving the performance of Li-S
2 batteries, we summarized the recent literature on the electrolyte additives published recently. As
3 can be seen in table S1, owing to the dual role of thiourea, the addition of only 0.2 M of this
4 additive to ether electrolytes, results in a stable cycling for 700 cycles, whereas other electrolyte
5 additives, improve the cycle life of Li-S battery for maximum of 500 cycles. Based on the results
6 presented, this study provides a good starting point for further research in designing electrolyte
7 additives with multiple roles.

8 **Associated Content**

9 The authors declare no competing financial interests.

10 **Corresponding Author**

11 *Email: vk99@drexel.edu

12 **Author Contributions**

13 The manuscript was written through the contributions of all authors. All authors have approved
14 the final version of the manuscript.

15 **Funding Sources**

1 This work was funded by the National Science Foundation (NSF-1804374, NSF- 1919177).

2 **Acknowledgment**

3 Authors acknowledge Dr. Jinwon Kim and Dr. Arvinder Singh for the insightful discussions,
4 the Materials Characterization Core at Drexel University for providing access to SEM and XRD.

5 We acknowledge Dr. Palmese's group for providing TGA.

6 **References**

- 7 1. A. Manthiram, Y. Fu, S.-H. Chung, C. Zu and Y.-S. Su, *Chemical reviews*, 2014, **114**,
8 11751-11787.
- 9 2. M. Wild, L. O'Neill, T. Zhang, R. Purkayastha, G. Minton, M. Marinescu and G. Offer,
10 *Energy & Environmental Science*, 2015, **8**, 3477-3494.
- 11 3. R. Demir-Cakan, 2017.
- 12 4. L. Borchardt, M. Oschatz and S. Kaskel, *Chemistry—A European Journal*, 2016, **22**, 7324-
13 7351.
- 14 5. A. Rafie, A. Singh and V. Kalra, *Electrochimica Acta*, 2021, **365**, 137088.
- 15 6. A. Singh and V. Kalra, *ACS applied materials & interfaces*, 2018, **10**, 37937-37947.
- 16 7. X. Liu, J. Q. Huang, Q. Zhang and L. Mai, *Advanced materials*, 2017, **29**, 1601759.
- 17 8. Q. Pang, X. Liang, C. Y. Kwok and L. F. Nazar, *Nature Energy*, 2016, **1**, 1-11.
- 18 9. R. Fang, J. Xu and D.-W. Wang, *Energy & Environmental Science*, 2020, **13**, 432-471.
- 19 10. R. Mukkabla and M. R. Buchmeiser, *Journal of Materials Chemistry A*, 2020, **8**, 5379-
20 5394.
- 21 11. N. Akhtar, X. Sun, M. Y. Akram, F. Zaman, W. Wang, A. Wang, L. Chen, H. Zhang, Y.
22 Guan and Y. Huang, *Journal of Energy Chemistry*, 2021, **52**, 310-317.
- 23 12. W. Yang, W. Yang, A. Song, L. Gao, G. Sun and G. Shao, *Journal of Power Sources*, 2017,
24 **348**, 175-182.
- 25 13. A. Singh, A. Rafie and V. Kalra, *Sustainable energy & fuels*, 2019, **3**, 2788-2797.

- 1 14. N. Angulakshmi and A. M. Stephan, *Frontiers in Energy Research*, 2015, **3**, 17.
- 2 15. Y. Tsao, M. Lee, E. C. Miller, G. Gao, J. Park, S. Chen, T. Katsumata, H. Tran, L.-W.
3 Wang and M. F. Toney, *Joule*, 2019, **3**, 872-884.
- 4 16. L. Zhang, M. Ling, J. Feng, L. Mai, G. Liu and J. Guo, *Energy Storage Materials*, 2018,
5 **11**, 24-29.
- 6 17. H.-L. Wu, M. Shin, Y.-M. Liu, K. A. See and A. A. Gewirth, *Nano Energy*, 2017, **32**, 50-
7 58.
- 8 18. F. Wu, J. T. Lee, N. Nitta, H. Kim, O. Borodin and G. Yushin, *Advanced Materials*, 2015,
9 **27**, 101-108.
- 10 19. J. Robinson, K. Xi, R. V. Kumar, A. C. Ferrari, H. Au, M.-M. Titirici, A. P. Puerto, A.
11 Kucernak, S. D. Fitch and N. Garcia-Araez, *Journal of Physics: Energy*.
- 12 20. Z. W. Zhang, H. J. Peng, M. Zhao and J. Q. Huang, *Advanced Functional Materials*, 2018,
13 **28**, 1707536.
- 14 21. Y. Chen, S. A. Freunberger, Z. Peng, O. Fontaine and P. G. Bruce, *Nature chemistry*, 2013,
15 **5**, 489.
- 16 22. S. Meini, R. Elazari, A. Rosenman, A. Garsuch and D. Aurbach, *The journal of physical*
17 *chemistry letters*, 2014, **5**, 915-918.
- 18 23. V.-C. Ho, D. T. Ngo, H. T. Le, R. Verma, H.-S. Kim, C.-N. Park and C.-J. Park,
19 *Electrochimica Acta*, 2018, **279**, 213-223.
- 20 24. C. Tran and V. Kalra, *Journal of Power Sources*, 2013, **235**, 289-296.
- 21 25. C. Dillard, S.-H. Chung, A. Singh, A. Manthiram and V. Kalra, *Materials today energy*,
22 2018, **9**, 336-344.
- 23 26. A. E. Bolzán and L. M. Gassa, *Journal of Applied Electrochemistry*, 2014, **44**, 279-292.
- 24 27. M. Mouanga and P. Bercot, *Int. J. Electrochem. Sci*, 2011, **6**, 1007-1013.
- 25 28. M. B. Q. Argañaraz, C. I. Vázquez and G. I. Lacconi, *Journal of Electroanalytical*
26 *Chemistry*, 2010, **639**, 95-101.
- 27 29. A. Bolzan, T. Iwasita and A. Arvia, *Journal of Electroanalytical Chemistry*, 2003, **554**, 49-
28 60.
- 29 30. J. Kirchnerová and W. C. Purdy, *Analytica Chimica Acta*, 1981, **123**, 83-95.
- 30 31. H. Uemachi, T. Sotomura, K. Takeyama and N. Koshida, *Journal*, 1995.

- 1 32. H. Tomkowiak and A. Katrusiak, *The Journal of Physical Chemistry C*, 2018, **122**, 5064-
2 5070.
- 3 33. A. Bhargav, J. He, A. Gupta and A. Manthiram, *Joule*, 2020, **4**, 285-291.
- 4 34. Y. V. Mikhaylik and J. R. Akridge, *Journal of the Electrochemical Society*, 2004, **151**,
5 A1969.
- 6 35. D. Moy, A. Manivannan and S. Narayanan, *Journal of the electrochemical society*, 2014,
7 **162**, A1.
- 8 36. C. Hu, H. Chen, Y. Shen, D. Lu, Y. Zhao, A.-H. Lu, X. Wu, W. Lu and L. Chen, *Nature*
9 *communications*, 2017, **8**, 1-9.
- 10 37. M. Xia, N. Zhang and C. Ge, *Journal of Materials Science*, 2020, 1-9.
- 11 38. Z. Wang, Y. Dong, H. Li, Z. Zhao, H. B. Wu, C. Hao, S. Liu, J. Qiu and X. W. D. Lou,
12 *Nature communications*, 2014, **5**, 1-8.
- 13 39. X. Wu, N. Liu, B. Guan, Y. Qiu, M. Wang, J. Cheng, D. Tian, L. Fan, N. Zhang and K.
14 Sun, *Advanced Science*, 2019, **6**, 1900958.
- 15 40. S. Li, D. Leng, W. Li, L. Qie, Z. Dong, Z. Cheng and Z. Fan, *Energy Storage Materials*,
16 2020, **27**, 279-296.
- 17 41. Y. Liu, Y. Pan, J. Ban, T. Li, X. Jiao, X. Hong, K. Xie, J. Song, A. Matic and S. Xiong,
18 *Energy Storage Materials*, 2020, **25**, 131-136.
- 19 42. Y. Song, W. Cai, L. Kong, J. Cai, Q. Zhang and J. Sun, *Advanced Energy Materials*, 2020,
20 **10**, 1901075.
- 21 43. M. Yu, Z. Wang, Y. Wang, Y. Dong and J. Qiu, *Advanced Energy Materials*, 2017, **7**,
22 1700018.
- 23 44. S. Megelski, J. S. Stephens, D. B. Chase and J. F. Rabolt, *Macromolecules*, 2002, **35**, 8456-
24 8466.
- 25 45. G. Xu, J. Yuan, X. Tao, B. Ding, H. Dou, X. Yan, Y. Xiao and X. Zhang, *Nano Research*,
26 2015, **8**, 3066-3074.
- 27 46. L. Yang, G. Li, X. Jiang, T. Zhang, H. Lin and J. Y. Lee, *Journal of Materials Chemistry*
28 *A*, 2017, **5**, 12506-12512.
- 29 47. S. Thieme, J. Brückner, A. Meier, I. Bauer, K. Gruber, J. Kaspar, A. Helmer, H. Althues,
30 M. Schmuck and S. Kaskel, *Journal of Materials Chemistry A*, 2015, **3**, 3808-3820.
- 31 48. M.-K. Song, Y. Zhang and E. J. Cairns, *Nano letters*, 2013, **13**, 5891-5899.

1 49. J. Liao and Z. Ye, *Batteries*, 2018, **4**, 22.

2

3

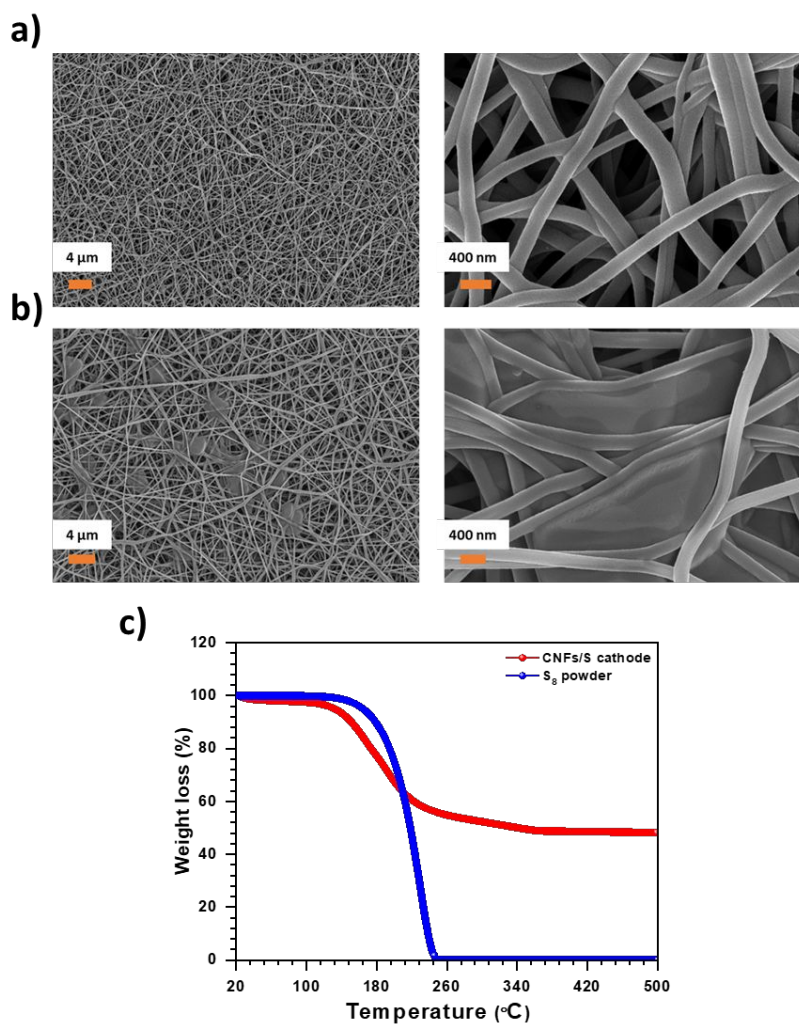
4

5

6

7

1 Figures:



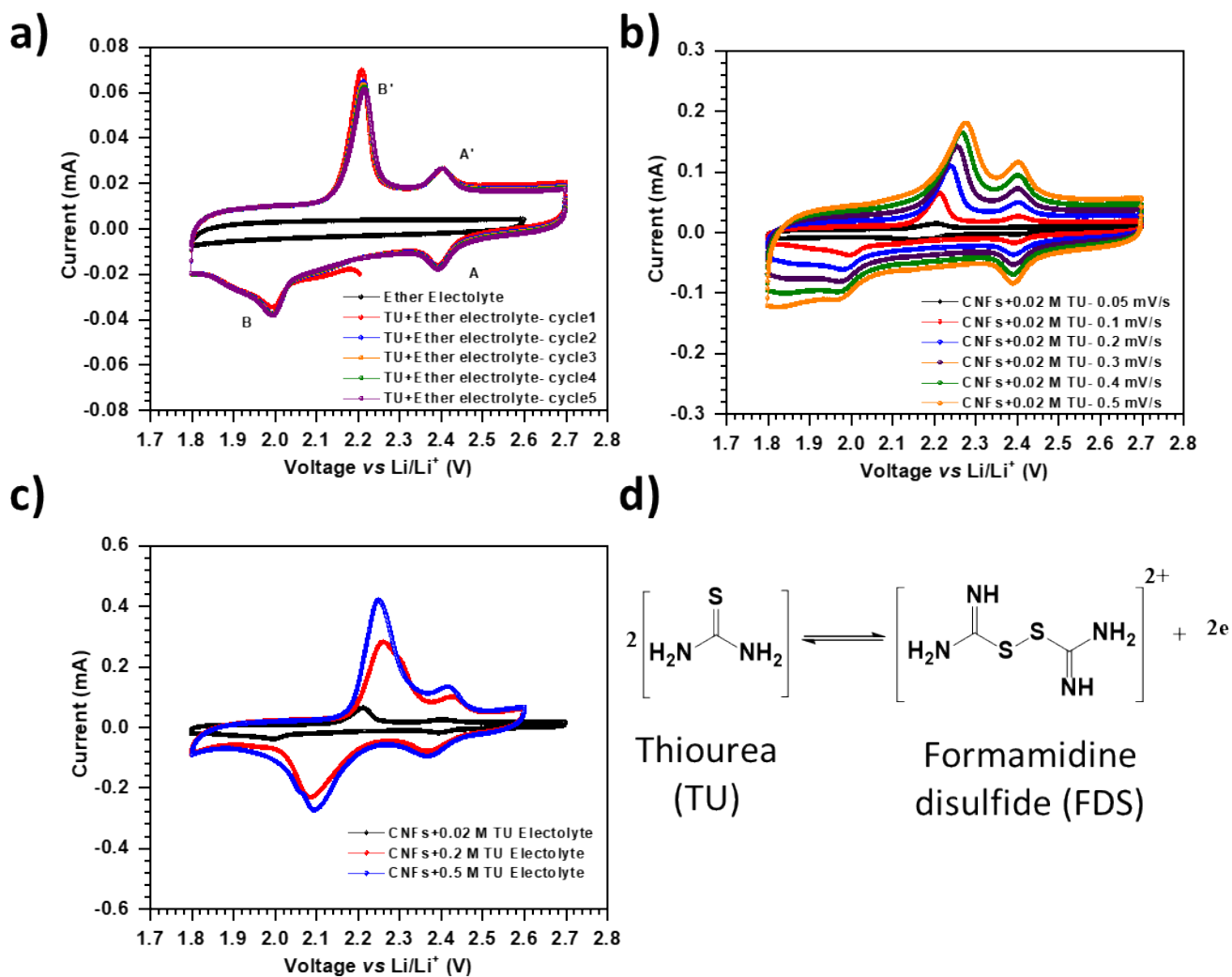
2

3

4 **Figure 1.** a) SEM image of CNFs, b) SEM image of SCNFs, sulfur is incorporated using the

5 ultra-rapid melt diffusion technique, and c) TGA result of sulfur powder and SCNF cathode used

6 in this study

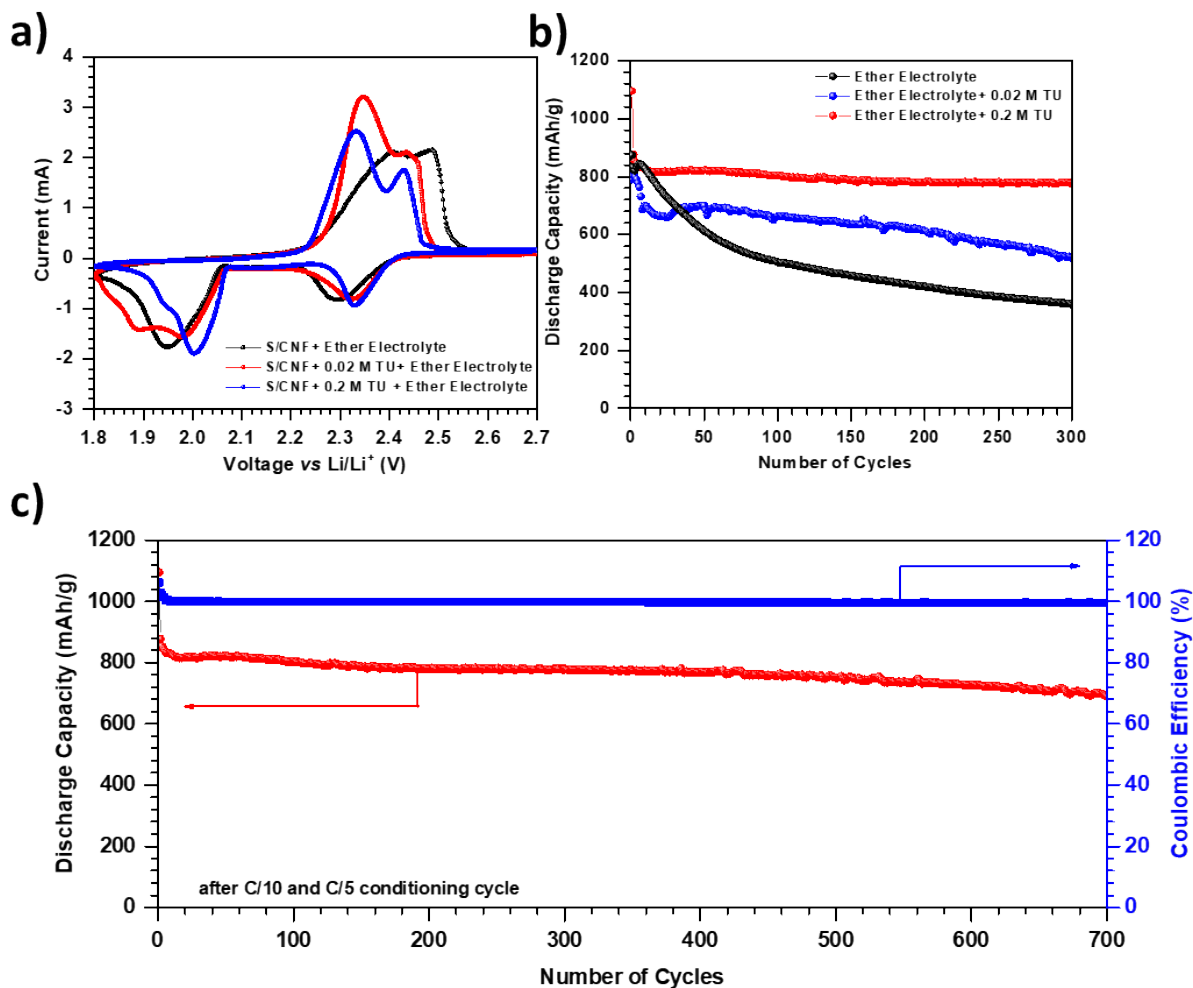


1
2
3 **Figure 2.** Cyclic voltammetry results of a) Blank cells – CNFs (without S), with and without TU
4 additive at 0.02 mV/s, b) CNFs with 0.02 M TU additive added to the electrolyte at different scan-
5 rates , c) CNFs when different concentration of TU (0.02, 0.2, and 0.5 M) was added to the ether-

1 based electrolyte, and f) proposed electrochemical pathway for redox activity of TU in ether-based

2 electrolyte

3



4

5 **Figure 3.a)** Cyclic voltammetry results SCNF cathodes, with and without TU additive at 0.02

6 mV/s, b) cycling results of SCNFs in ether-based electrolyte, compared to when 0.02 M TU and

1 0.2 M TU is added to the ether-based electrolyte, and c) long-term cycling and coulombic
2 efficiency results of 0.2 M TU in ether electrolyte

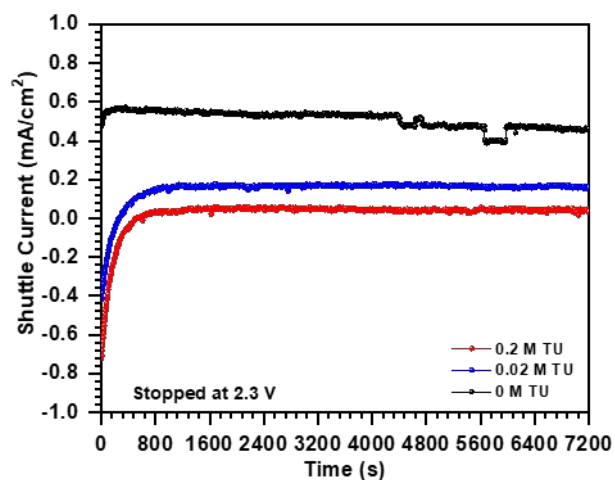
3

4

5

6

7



8

9 **Figure 4.** Steady-state shuttle current measurement at 2.3 V with and without TU electrolyte and

10

11

1

2

3

4

5

6

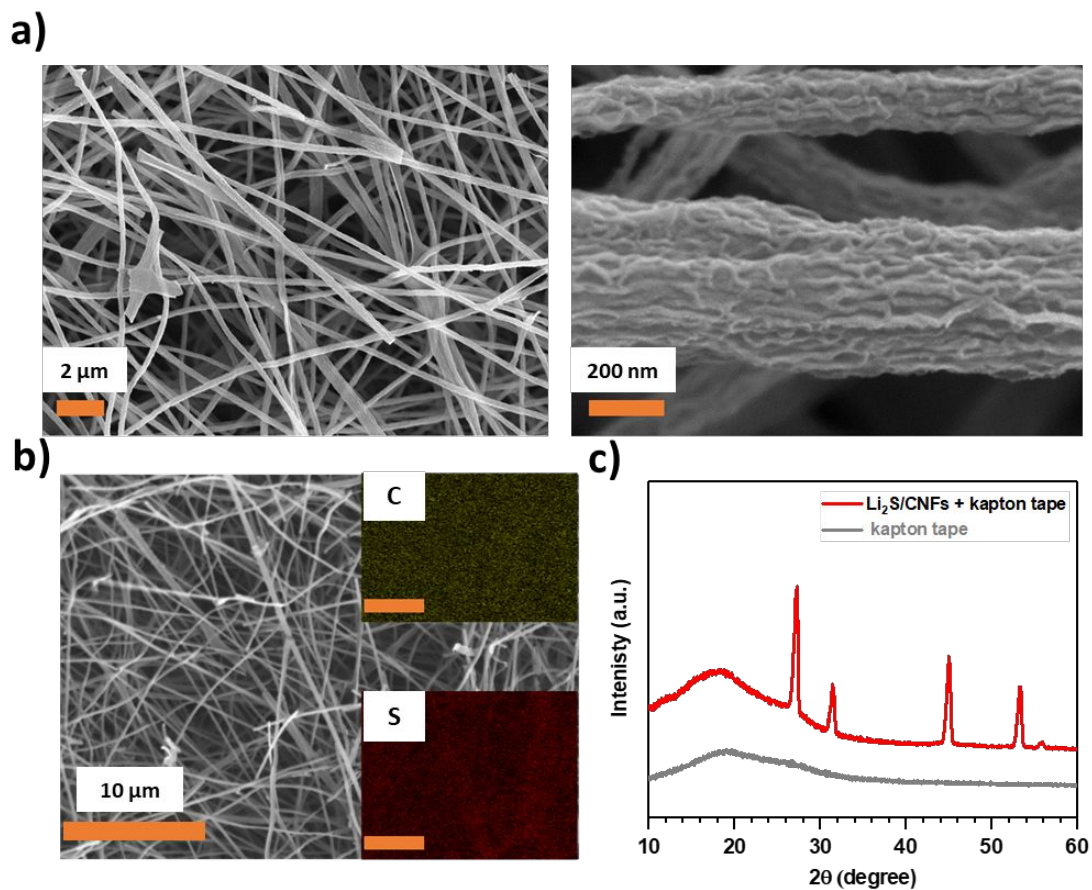
7

8

9

10

11



1
 2 **Figure 5.** a) SEM image of Li₂S/CNF cathode fabricated using electrospinning technique, b)
 3 SEM picture and elemental mapping of Li₂S/CNF cathode, and c) XRD result of Li₂S/CNF sealed
 4 with Kapton tape and XRD of Kapton tape for reference

5

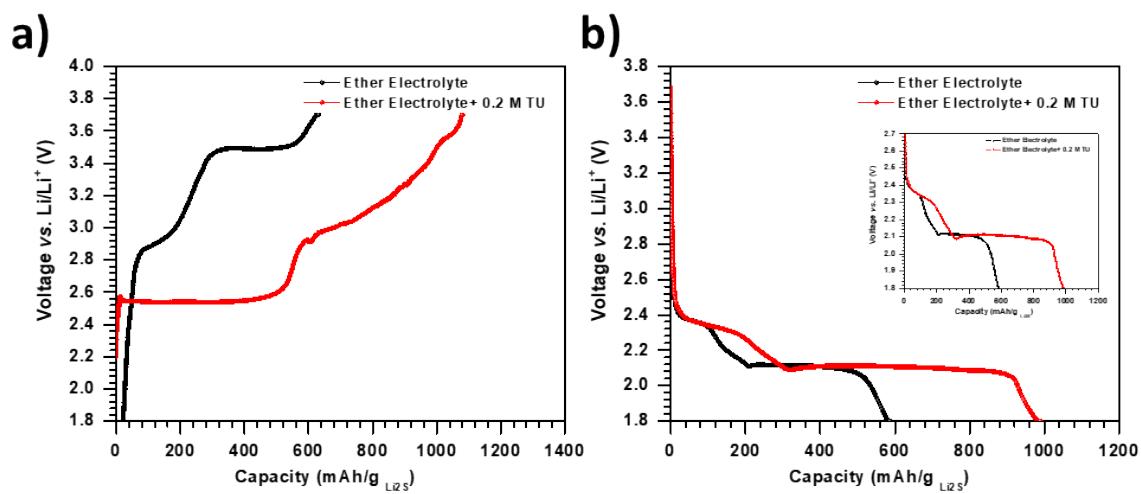
6

7

8

1

2



3

4 **Figure 6.** a) Galvanostatic charge-discharge plot for first charge half cycle of $\text{Li}_2\text{S}/\text{CNF}$ cathode5 at $C/20$, and b) Charge-discharge curves of subsequent discharge step of $\text{Li}_2\text{S}/\text{CNF}$ cathode at6 $C/20$, inset is zoomed in between 1.8 to 2.7 V,

7

8

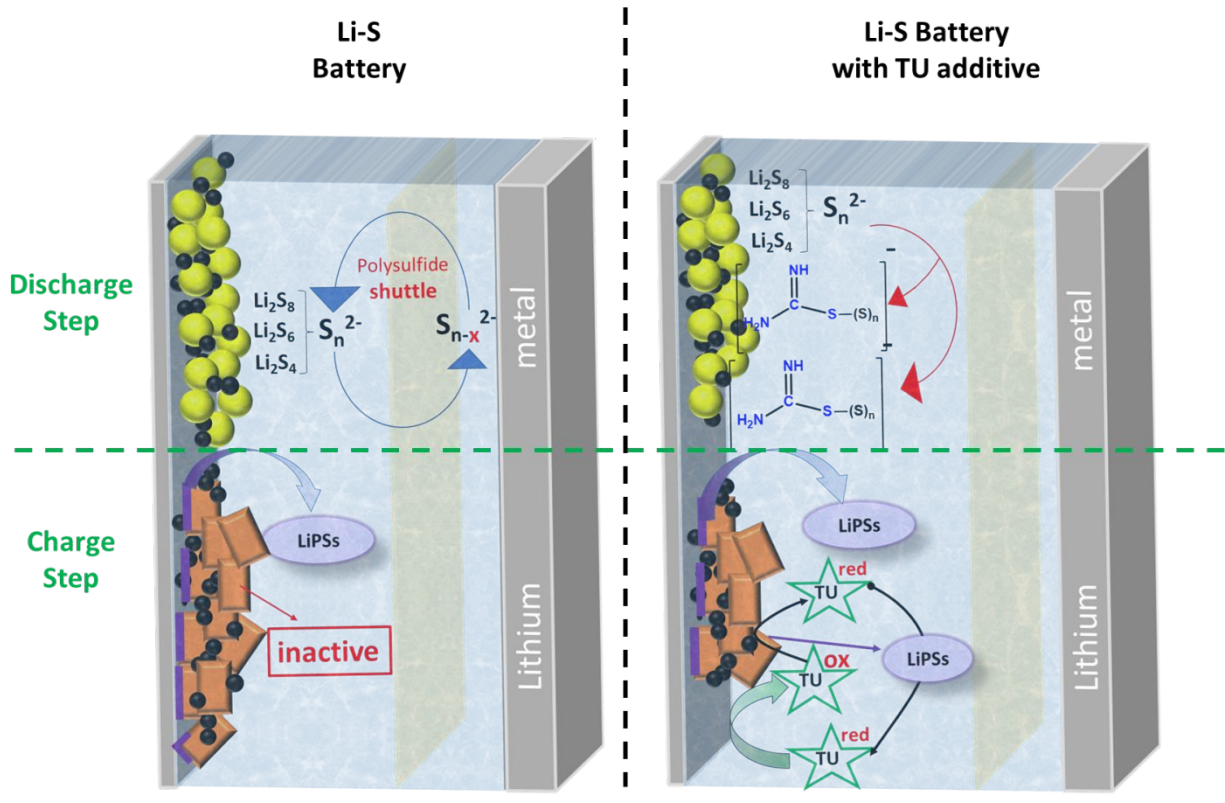
9

10

11

12

1
2
3
4
5
6
7

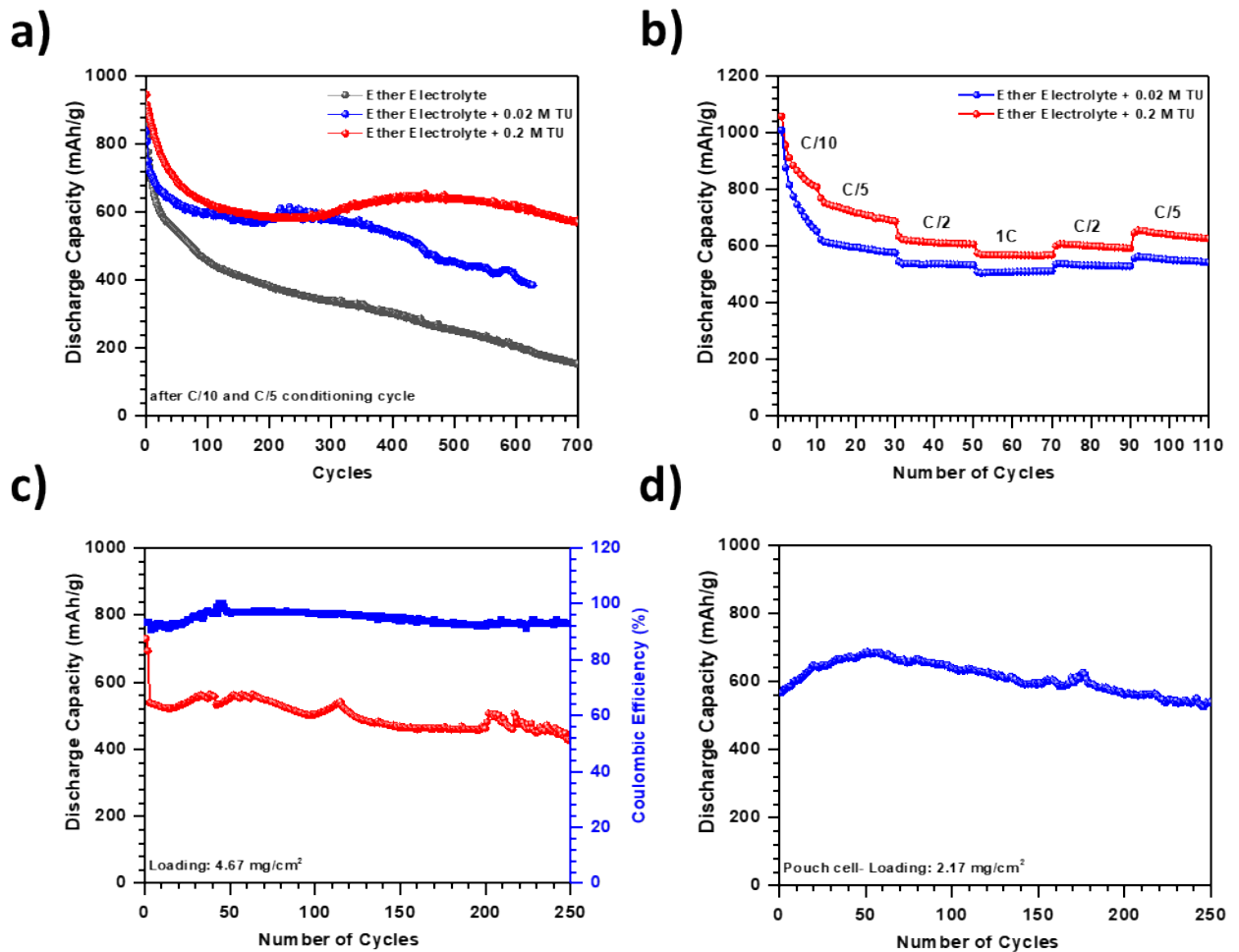


8

1 **Schematic 1.** The role of TU as an electrolyte additive in reducing polysulfide shuttling in
 2 discharge step and redox mediator in charge step

3

4



5

6 **Figure 7.** a) A comparison between the long term cycling results of slurry sulfur cathode in
 7 ether-based electrolyte with and without TU additive at C/2 rate, b) rate-capability test of Li-S

- 1 batteries using slurry cathodes and TU electrolyte additive at different C-rates, c) cycling results
- 2 for slurry cathode with high loading of ~ 4.7 mg/cm², with 0.2M TU added to ether-based
- 3 electrolyte at C/5 rate, and d) cycling result of pouch cell level Li-S battery with 0.2 M TU at C/5
- 4 rate
- 5
- 6